



## Short communication

Preparation of Cu<sub>2</sub>O/TiO<sub>2</sub> composite porous carbon microspheres as efficient visible light-responsive photocatalystsGuohua Jiang<sup>a,b,\*</sup>, Rijing Wang<sup>a,b</sup>, He Jin<sup>c</sup>, Yin Wang<sup>a,b</sup>, Xinke Sun<sup>a,b</sup>, Sheng Wang<sup>a,b</sup>, Tao Wang<sup>a,b</sup><sup>a</sup> Department of Materials Engineering, College of Materials and Textile, Zhejiang Sci-Tech University, Hangzhou 310018, PR China<sup>b</sup> Key Laboratory of Advanced Textile Materials and Manufacturing Technology (ATMT), Ministry of Education, Zhejiang Sci-Tech University, Hangzhou 310018, PR China<sup>c</sup> Qixin Honors College, Zhejiang Sci-Tech University, Hangzhou 310018, PR China

## ARTICLE INFO

## Article history:

Received 10 December 2010

Received in revised form 27 March 2011

Accepted 22 April 2011

Available online 8 May 2011

## Keywords:

Composite materials

Heat treatment

Electron microscopy

Microstructure

## ABSTRACT

In this paper, Cu<sub>2</sub>O/TiO<sub>2</sub> composite porous microspheres were prepared in the absence of templates and additives by a simple hydrothermal method using Cu(CH<sub>3</sub>COO)<sub>2</sub>·H<sub>2</sub>O and (NH<sub>4</sub>)<sub>2</sub>TiF<sub>6</sub> as precursors. The photocatalytic activity of the samples was evaluated by the photo-degradation of methylene blue (MB) aqueous solution under the visible-light illumination. To the best of our knowledge, this is the first report on the preparation and photocatalytic activity of Cu<sub>2</sub>O/TiO<sub>2</sub> composite porous microspheres with a template-free hydrothermal method. This work may provide new insights into preparing other inorganic porous microspheres.

© 2011 Elsevier B.V. All rights reserved.

## 1. Introduction

Recently, there has been considerable interest in the synthesis of micrometer- and nanometer-sized porous spheres because of their widespread potential applications in catalysis, drug delivery, chromatography separation, chemical reactors, controlled release of various substances, and protection of environmentally sensitive biological molecules [1–5]. Among various synthesis methods, template-directed approaches have been demonstrated to be effective for preparing hollow microspheres. Various methods using hard templates (e.g., polymer latex, carbon, anodic aluminum oxide templates) or soft templates (e.g., supramolecular, ionic liquids, surfactant, organogel) have been extensively investigated [6–10]. These methods often involve the coating of nanocrystals on the template surface, followed by removal of the template using calcination or etching. The latter processes often compromise the structural integrity of the final product and so limit the application of the template-directed approach. In addition, using well-known physical phenomena such as the Kirkendall effect and Ostwald ripening, researchers have fabricated various hollow or porous nanostructures such as TiO<sub>2</sub>, SrTiO<sub>3</sub>, BaTiO<sub>3</sub>, etc, in the presence of templates [11–16]. However, in general, it remains a major challenge to develop a facile, template-free, one-step solution route for the preparation of inorganic porous nanostructures.

TiO<sub>2</sub> is a very important multifunctional material because of its peculiar and fascinating physicochemical properties and a wide variety

of potential uses in diverse fields such as solar energy conversion, environmental purification, water treatment and antibacterial materials [16–19]. However, the high energy band gap of pure TiO<sub>2</sub> ( $E_g = 3.0$  eV for rutile,  $E_g = 3.2$  eV for anatase) limits its application because the electron–hole pairs can only be formed by UV light at wavelength shorter than 387 nm [20, 21]. Thus, only a small portion of the solar spectrum can be utilized for photo-oxidation reaction using TiO<sub>2</sub>. Additionally, the electrons and holes will undergo recombination rapidly, estimated at a rate of  $(3.2 \pm 1.4) \times 10^{-11} \text{ cm}^3 \text{ s}^{-1}$ , if they are not consumed upon generation. The high electron/hole pair recombination rate reduces the quantum yield which is another major drawback in heterogeneous photocatalysis using TiO<sub>2</sub>. In order to improve the solar conversion efficiency, there are great efforts that have been made to extend the useful response of this TiO<sub>2</sub>-based material to the visible region, the method including dye sensitization, non-metal or transition metal ions doping and surface modification. Although there are many ways to improve visible light absorption, only a very limited cases reported so far have shown significant visible activity, and the most systems suffer from rapid charge recombination, the thermal or photochemical instability of the defect materials. It has been reported that CuO and Cu<sub>2</sub>O, p-type semiconductors, have narrow band gaps ( $E_g$  (CuO) = 1.2 eV and  $E_g$  (Cu<sub>2</sub>O) = 2.0 eV) [22]. CuO has been widely exploited for diverse applications as heterogeneous catalysts, gas sensors, superconductors, optical switches, lithium ion electrode materials, and field-emission emitters, whereas Cu<sub>2</sub>O has been used in solar energy conversion, catalysis, electronics, and magnetic storage. However, Cu<sub>2</sub>O/TiO<sub>2</sub> composites with porous nanostructures and their photocatalytic activity were seldom reported in these previous studies. In this paper, Cu<sub>2</sub>O/TiO<sub>2</sub> composite porous microspheres were prepared

\* Corresponding author at: Department of Materials Engineering, College of Materials and Textile, Zhejiang Sci-Tech University, Hangzhou 310018, PR China. Tel.: +86 571 86 843527. E-mail address: [polymer\\_jiang@hotmail.com](mailto:polymer_jiang@hotmail.com) (G. Jiang).

by a simple hydrothermal method without assistance of any templates. The photocatalytic activity of the samples was evaluated by the photo-degradation of methylene blue (MB) aqueous solution under the visible-light illumination.

## 2. Experimental

### 2.1. Materials

Analytical grade glucose was purchased from Beijing Chemical Corporation and used as the starting materials without further purification. Cupric acetate ( $\text{Cu}(\text{CH}_3\text{COO})_2 \cdot \text{H}_2\text{O}$ ) and ammonium fluotitanate ( $(\text{NH}_4)_2\text{TiF}_6$ ) obtained were purchased from Shanghai Chemical Co., Ltd. MB aqueous solution was prepared by dissolved methylene blue (obtained from Sigma-Aldrich Inc.) in distilled water with concentration ( $\rho$ ) at 30 mg/L.

### 2.2. Preparation

The composite microspheres were prepared according to the modified method described in the previous literature [16]. 0.5 g of  $\text{Cu}(\text{CH}_3\text{COO})_2 \cdot \text{H}_2\text{O}$  and 1.5 g of  $(\text{NH}_4)_2\text{TiF}_6$  were dissolved in 60 mL distilled water to prepare the precursor solution. Subsequently, glucose (8.0 g) was added into the precursor solution. The solution was then sealed in a 100 mL Teflon-lined stainless steel autoclave and maintained at 160 °C. After reaction for 24 h, the powder precipitates are filtered, rinsed with distilled water and ethanol three times, respectively, and dried in a vacuum oven at 60 °C for 8 h. The final products were obtained through a heat-treatment at desired temperatures in the air for 1 h with a heating rate of 2 °C/min.

### 2.3. Characterization

The morphology and microstructure of  $\text{Cu}_2\text{O}/\text{TiO}_2$  composite porous microspheres were characterized with SEM (scanning electron microscopy, HITACHI S-4800 instrument, Japan). XRD patterns were analyzed by using X-ray diffractometer (i.e. SIEMENS Diffraktometer D5000, Germany) using  $\text{Cu K}\alpha$  radiation source at 35 kV, with a scan rate of 0.02°. Crystallite size of anatase  $\text{TiO}_2$  can be determined from the line broadening by using Scherrer's formula. Thermogravimetric analysis (TGA) was performed on a Pyris Diamond 1 instrument (America) at a heating rate of 20 °C/min from 25 °C to 600 °C in a flow of nitrogen. The UV–Vis spectra were measured by a JASCO V-570 UV/Vis/NiR spectrophotometer (made by JASCO Corporation, Japan). The Brunauer–Emmet–Teller (BET) specific surface area ( $S_{\text{BET}}$ ) of the samples was determined by a high speed automated area and pore size analyzer (F-Sorb3400, China).

### 2.4. Measurement of photocatalytic activity

The photo-degradation experiments were carried out in open box, whose light radiation source is 50 W daylight lamp with a distance of 2-meter. The photo-reactor consisted of two 100 mL beakers, which filled with 80 mL aqueous MB solution and photo-catalysts suspension, and magnetically stirred. No pure oxygen was supplied because it has enough oxygen for oxidation photo-degradation under continuously stirring in atmosphere in previous experiment [23, 24].

The initial methylene blue (MB) concentration ( $\rho_0$ ) was 30 mg/L, the photo-catalyst concentration was 1 g/L, and the pH of the solution was adjusted to 1.7, 7.0 and 10.0 with ammonia and nitric acid solution, and measured clear solution concentration by JASCO V-570 UV/Vis/NiR spectrophotometer at  $\lambda_{\text{max}} = 546$  nm wavelength, the  $\rho_0$  was considered as beginning concentration before adding catalyst. The samples were withdrawn regularly from the beakers. The MB concentrations ( $\rho_i$ ) in different times were obtained and the degradation rate could be expressed as the following formula.

Degradation rate:

$$R = (\rho_0 - \rho_i) / \rho_0 \times 100\%.$$

## 3. Results and discussion

The main process in this green method was carried out in aqueous condition without the use of organic solvents or etching agents [23]. Hierarchically  $\text{Cu}_2\text{O}/\text{TiO}_2$  composite microspheres are prepared in the absence of templates and additives by a simple hydrothermal method using  $\text{Cu}(\text{CH}_3\text{COO})_2 \cdot \text{H}_2\text{O}$  and  $(\text{NH}_4)_2\text{TiF}_6$  as precursors. The XRD patterns of as-prepared sample and calcined samples at 200 °C, 300 °C and 400 °C for an hour are shown in Fig. 1. The  $\text{Cu}_2\text{O}$  doped  $\text{TiO}_2$  composite was not obtained directly, and the product obtained by the solvothermal reaction exhibited mixed phases; the majority of the diffraction peaks could be indexed to the Cu phase and the diffraction peaks with low intensities and wide range corresponded to amorphous carbon phase. The solvothermal product was calcined at 200 and 300 °C to obtain  $\text{Cu}_2\text{O}$  and CuO doped  $\text{TiO}_2$  composites. At higher heat treatment temperature, higher content of  $\text{Cu}_2\text{O}$  in the sample can be obtained.  $\text{Cu}_2\text{O}$  can be fabricated by the redox reaction of CuO with Cu as the reduction agent at high temperature in the air [24, 25]. The redox reaction can be shown as:



Fig. 2 shows the morphological information of the solvothermal product and calcined samples. The as-prepared sample showed a large number of highly uniform microspheres with diameters ranging from 1 to 3  $\mu\text{m}$  (Fig. 1A). The surface of the as-prepared sample is very smooth as shown in Fig. 1A. The morphology of the sample treated by heat at 200 °C is almost no change with the as-prepared product (Fig. 1B). However, increasing the temperature for heat-treatment, the surface morphology of microspheres changed from smooth to porous structure. Few holes can be found in the calcined samples with treatment at 300 °C (Fig. 1C) and the porous surface structure can be obtained in the calcined samples with treatment at 400 °C (Fig. 1D) for an hour. Under higher temperature, the carbon can be removed from microspheres in the form of carbon dioxide which departed from the core through the shell, resulting in the formation of porous structure on the microspheres' surface [26, 27]. Prolonging the heat treatment time, the carbon in the microspheres can be removed completely, and metal oxide nanoparticles with diameter around 20–30 nm are left, which was confirmed by the TEM as shown in Fig. 3.

Fig. 4 shows the TGA of the as-prepared and calcined microspheres. It can be seen that the weight loss temperatures for two

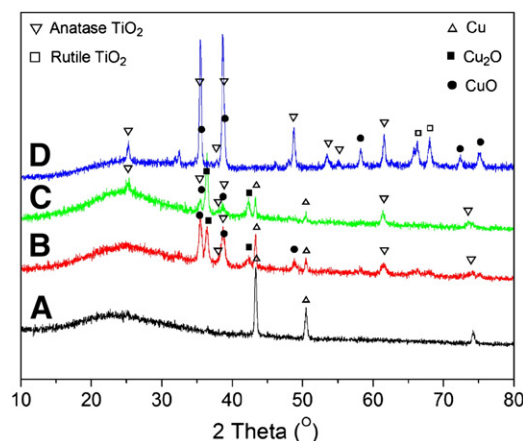


Fig. 1. XRD patterns of as-prepared composite microspheres (A) and the samples with treatments at 200 °C (B), 300 °C (C) and 400 °C (D) for an hour.

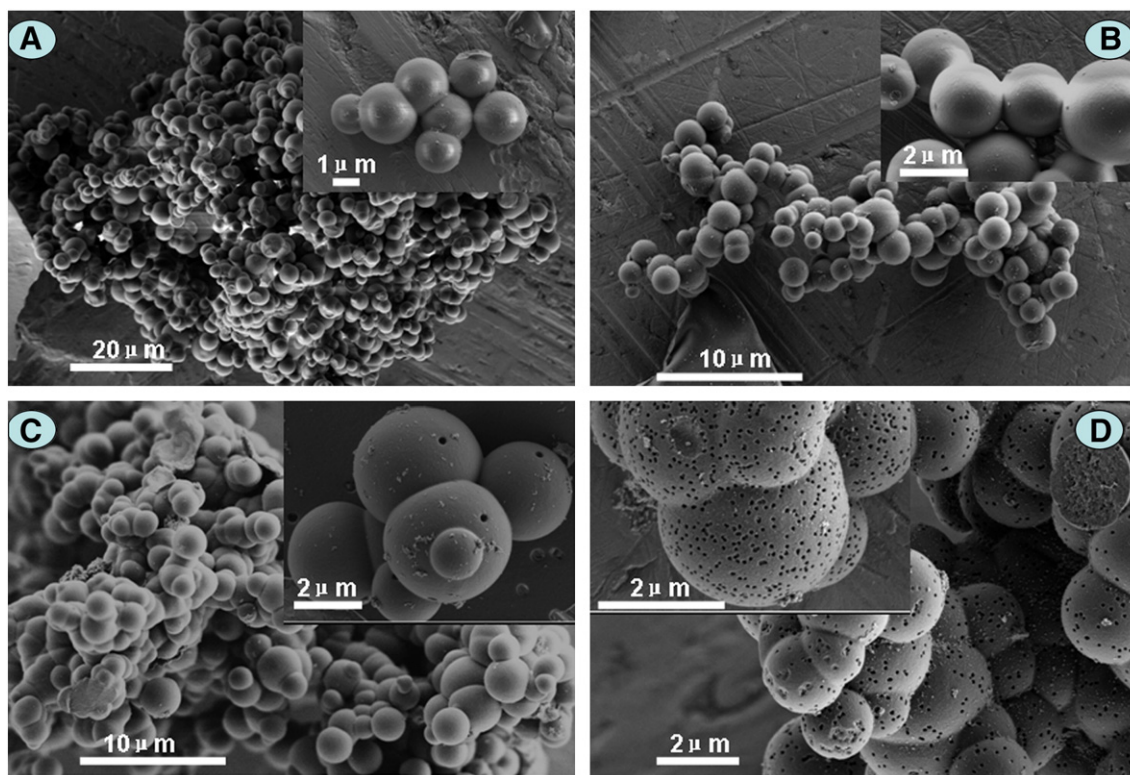


Fig. 2. FESEM images of solvothermal product (A) and calcined samples with heat treatment at 200 °C (B), 300 °C (C) and 400 °C (D) for an hour.

samples are obviously different. For the as-prepared sample, the first weight loss is centered at 50 °C, which can be attributed to desorption of physically adsorbed water. The second large weight loss is centered at 400 °C, which corresponds to the removal of carbon in the microspheres as shown in Fig. 4A. Hence, the porous microspheres can be obtained for the as-prepared microspheres with calcination at 400 °C. For the calcined sample, the second large weight loss is centered at 500 °C, which also corresponds to the removal of carbon in the microspheres as shown in Fig. 4B. However, the higher weight loss temperature may be attributed to the higher thermal stability and lower carbon content in the microsphere. The residual weight percent for the calcined sample is higher than that of the as-prepared sample.

UV–Vis absorption spectrum of the prepared  $\text{Cu}_2\text{O}$  doped composite porous carbon microsphere sample is shown in Fig. 5A. The spectrum shows red-shift in the band gap transition compared to the pure  $\text{TiO}_2$  [16] and the absorption edge shift to visible region is

caused by  $\text{Cu}_2\text{O}$  content. With regard to the results from XRD analysis, it could be concluded that  $\text{Cu}_2\text{O}$  doping led to decrease band gap energies and visible-light activation [28]. The method of UV/Vis diffuse reflectance spectroscopy was employed to estimate band gap energies of the  $\text{Cu}_2\text{O}$  doped composite porous carbon microsphere sample. First, to establish the type of band-to-band transition in the synthesized particles, the absorption data were fitted to equations for direct band gap transitions. The minimum wavelength required to promote an electron depends upon the band gap energy  $E_{\text{bg}}$  of the photocatalyst and is given by:  $E_{\text{bg}} = 1240/\lambda$  (eV), where  $\lambda$  is the wavelength in nanometers [29, 30]. Fig. 5B shows the  $(\alpha E_{\text{bg}})^2$  versus  $E_{\text{bg}}$  for an indirect band gap transition of  $\text{Cu}_2\text{O}$  doped composite where  $\alpha$  is the absorption coefficient and  $E_{\text{bg}}$  is the photon energy. The value of  $E_{\text{bg}}$  extrapolated to  $\alpha = 0$  gives an absorption energy that corresponds to a band-gap energy. Estimating from the intercept of the tangents to the plots, the direct band gap energy for the sample

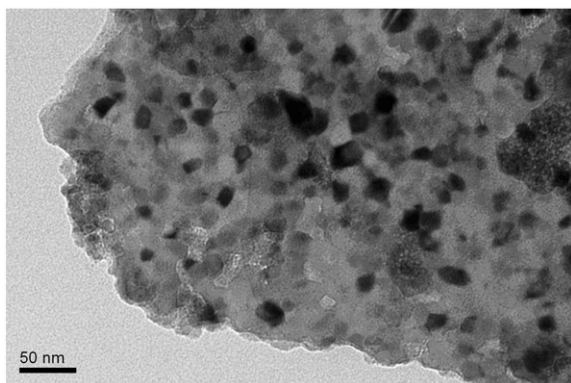


Fig. 3. TEM image of calcined samples with heat treatment at 500 °C for an hour.

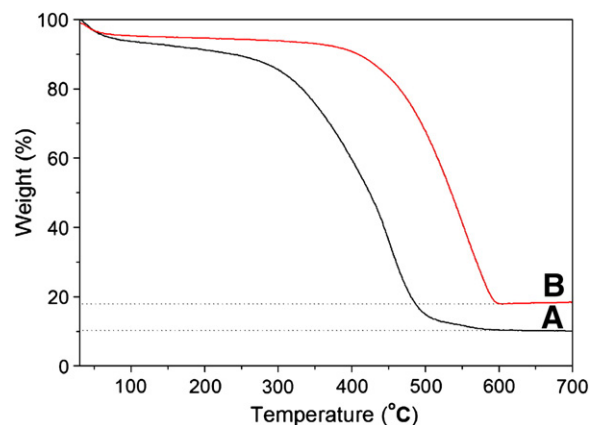


Fig. 4. TGA of the as-prepared (A) and calcined microspheres (B, 400 °C for an hour).

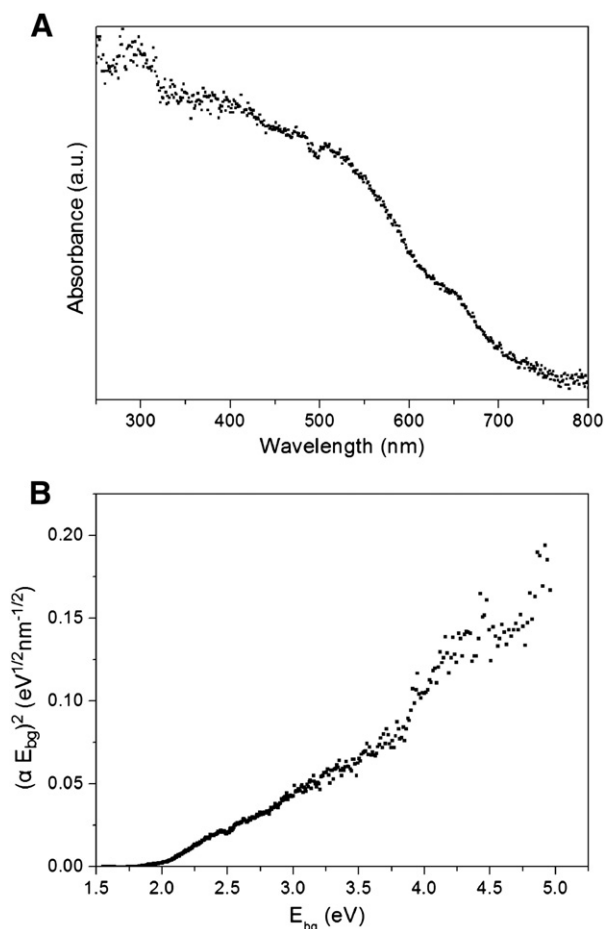


Fig. 5. Diffuse reflectance spectrum (A) and band-gap energy (B) of calcined microspheres (400 °C for an hour).

was 2.0 eV, which is attributed to Cu<sub>2</sub>O content in the composite [22]. This result obviously revealed that the band gap of the sample was narrower than that of the pure TiO<sub>2</sub>.

Specific surface area is a significant surface parameter for the Cu<sub>2</sub>O/TiO<sub>2</sub> composite porous microspheres. The composite microspheres were prepared without further calcination treatment with a specific surface area of 0.363 m<sup>2</sup> g<sup>-1</sup>. Interestingly, the composite microspheres show the higher specific surface area with higher temperature treatment as shown in Fig. 6A. The samples have the specific surface areas of 65.081, 114.845 and 126.377 m<sup>2</sup> g<sup>-1</sup> for calcination treatments at 200, 300 and 400 °C, respectively. The presence of porous structure on the surface of the composite microspheres helps to enlarge the specific surface area of resultant samples significantly which leads to their higher adsorptive ability. The change of pore diameter for the composite microspheres shows the similar trend as the specific surface area. The bigger pore diameter at higher calcination treatment can be observed as shown in Fig. 6B.

Photo-catalytic property of the prepared samples was evaluated by the degradation of methylene blue (MB) at atmospheric pressure using composite porous microsphere samples (heat treatment at 400 °C for an hour). Fig. 7 shows the photo-catalytic degradation of MB against residence time. It is clear from the figure that the rate of photo-catalytic degradation of MB is higher at the neutral and alkaline environment. 50% of MB can be degraded in 2 h for three pH conditions. Almost all MB can be degraded at the neutral and alkaline environment after reaction for 24 under visible light irradiation. However, about 20% of MB has not been degraded in the acidic condition. The inset in Fig. 6 shows the digital illumination photographs of MB aqueous solution under visible light irradiation

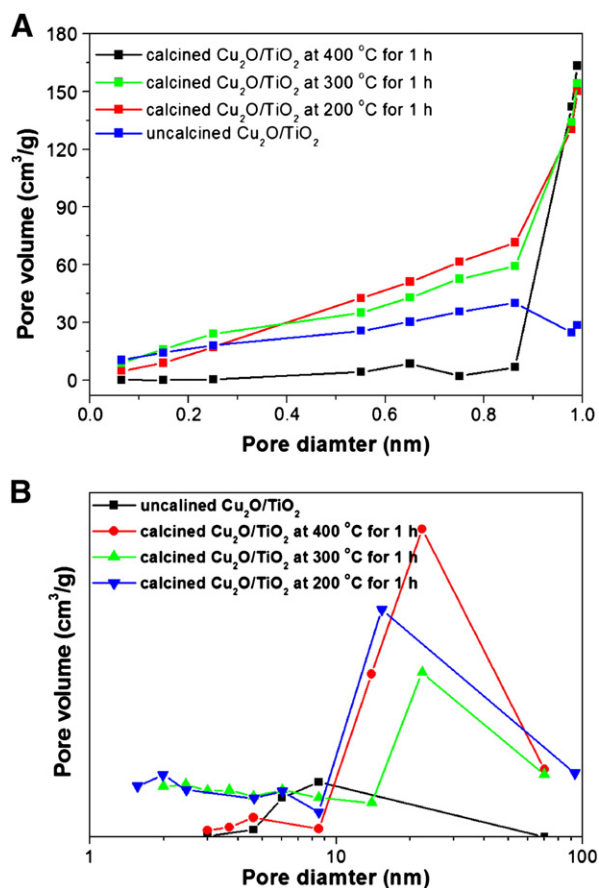


Fig. 6. Specific surface area and pore size data for the products with or without heat treatment.

at different pH values. At pH = 10.0 and 7.0, the color of solution fades gradually with extension of irradiation time. While, it has almost no great change in color after reaction for 2 h at pH = 1.7. The reason for this is that the pH influences the adsorption property of organic compounds and their dissociating state in solution. It is well known that the surface defects of metal oxides nanostructures function as MB adsorption sites in the solution. Meanwhile the large surface area of the mesoporous structures is able to further enhance the sensitivity to

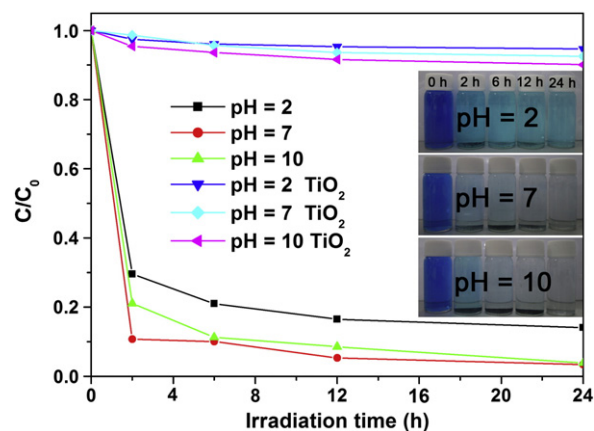


Fig. 7. The photo-catalytic degradation of MB with composite microspheres and pure TiO<sub>2</sub> against residence time ( $C_{MB} = 30$  mg/L,  $C_{catalyst} = 1$  g/L) and digital illumination photographs of MB aqueous solution under visible light irradiation at different pH values (inset).

white light and might even lead to the realization of single photon detection. However, for the pure TiO<sub>2</sub> sample (P-25, Degussa AG, Germany), no significant degradation of MB at all three pH conditions are observed. The reason for this phenomenon is that the electron–hole pairs cannot be formed under the visible light irradiation for the high energy band gap of pure TiO<sub>2</sub>.

#### 4. Conclusion

Cu<sub>2</sub>O/TiO<sub>2</sub> composite porous microspheres were prepared in the absence of templates and additives by a simple hydrothermal method using Cu(CH<sub>3</sub>COO)<sub>2</sub>·H<sub>2</sub>O and (NH<sub>4</sub>)<sub>2</sub>TiF<sub>6</sub> as precursors. Because of Cu<sub>2</sub>O doping in the composite microspheres which led to decrease band gap energies and visible-light activation, the Cu<sub>2</sub>O/TiO<sub>2</sub> composite porous microspheres showed visible light-responsive photo-catalytic property for degradation of methylene blue (MB) aqueous solution under the visible-light illumination. This work may provide new insights into preparing other inorganic hollow microspheres and may extend potential applications for degradation of organic pollutants.

#### Acknowledgments

This work was financially supported by the Qianjiang Talents Project of Zhejiang Province (2010R10023), the Scientific Research Foundation for the Returned Overseas Chinese Scholars, the State Education Ministry (1001603-C), the Natural Science Foundation of Zhejiang Province (Y4100045, Y4080392, R210101054), the Key Bidding Project of Zhejiang Provincial Key Lab of Fiber Materials and Manufacturing Technology, Zhejiang Sci-Tech University (S2010002), the Natural Science Foundation of China (31070888, 50802088) and the Program for Changjiang Scholars and Innovative Research Team in University (PCSIRT: 0654). H. J. thanks the Xinmiao Talent program of Zhejiang Province for financial support.

#### References

- [1] X.L. Zeng, P. Wu, F.L. Luo, C. Zhou, D.G. Tong, *J. Phys. Chem. Solid.* 71 (2010) 1404–1409.
- [2] L. Kong, G.O. Duan, G. Zuo, W. Cai, Z. Cheng, *Mater. Chem. Phys.* 123 (2010) 421–426.
- [3] J.J. Kirkland, *J. Chromatogr.* 125 (1976) 231–250.
- [4] J. Hanes, M. Chiba, R. Langer, *Biomaterials* 19 (1998) 163–172.
- [5] Y. Zhu, L. Zhang, F.M. Schappacher, R. Poettgen, J. Shi, K. Stefan, *J. Phys. Chem C.* 112 (2008) 8623–8628.
- [6] Q. Liu, L. Wang, A. Xiao, J. Gao, W. Ding, H. Yu, J. Huo, M. Ericson, *J. Hazard. Mater.* 181 (2010) 586–592.
- [7] D.G. Shchukin, R.A. Caruso, *Chem. Commu.* 13 (2003) 1478–1479.
- [8] S. Lei, K. Tang, Y. Qi, Z. Fang, H. Zheng, *Europ. J. Inorg. Chem.* 12 (2006) 2406–2410.
- [9] J. Liu, F. Liu, K. Gao, J. Wu, D. Xue, *J. Mater. Chem.* 19 (2009) 6073–6084.
- [10] Y. Deng, C. Liu, T. Yu, F. Liu, F. Zhang, Y. Wan, L. Zhang, C. Wang, B. Tu, P.A. Webley, H. Wang, D. Zhao, *Chem. Mater.* 19 (2007) 3271–3277.
- [11] W.-S. Wang, L. Zhen, C.-Y. Xu, J.-Z. Chen, W.-Z. Shao, *Appl. Mater. Interfaces* 1 (2009) 780–788.
- [12] L. Kong, X. Lu, X. Bian, W. Zhang, C. Wang, *J. Solid State Chem.* 183 (2010) 2421–2425.
- [13] J.-Y. Zhang, H.-Q. Yang, Y.-Z. Song, D.-C. Chen, L. Li, H. Jiao, L.-F. Wang, *Acta Chim. Sinica* 65 (2007) 2069–2075.
- [14] Y. Qi, K. Tang, S. Zeng, W. Zhou, *Microporous Mesoporous Mater.* 114 (2008) 395–400.
- [15] M.K. Devaraju, S. Yin, T. Sato, *Cryst. Growth Des.* 9 (2009) 2944–2949.
- [16] J. Yu, W. Liu, H. Yu, *Cryst. Growth Des.* 8 (2008) 930–934.
- [17] G. Jiang, J. Zeng, *J. Appl. Polym. Sci.* 116 (2010) 779–784.
- [18] G. Jiang, X. Zheng, Y. Wang, T. Li, X. Sun, *Powder Technol.* 207 (2011) 465–469.
- [19] J. Ryu, W. Choi, *Environ. Sci. Technol.* 42 (2008) 294–300.
- [20] B. Zhou, X. Zhao, H. Liu, J. Qu, C.P. Huang, *Appl. Catal. B* 99 (2010) 214–221.
- [21] W. Choi, A. Termin, M.R. Hoffmann, *J. Phys. Chem.* 98 (1994) 13669–13679.
- [22] H. Yu, J. Yu, S. Liu, S. Mann, *Chem. Mater.* 19 (2007) 4327–4334.
- [23] G. Jia, M. Yang, Y. Song, H. You, H. Zhang, *Cryst. Growth Des.* 9 (2009) 301–307.
- [24] S.H. Chen, H.-Y. Chu, Y.-B. Shih, C. Han, *J. Vac. Sci. Technol. B* 23 (2005) 2557–2560.
- [25] W. Wang, O.K. Varghese, C. Ruan, M. Paulose, C.A. Grimes, *J. Mater. Res.* 18 (2003) 2756–2759.
- [26] S. Wang, J. Zhang, J. Jiang, R. Liu, B. Zhu, M. Xu, Y. Wang, J. Cao, M. Li, Z. Yuan, S. Zhang, W. Huang, S. Wu, *Microporous Mesoporous Mater.* 123 (2009) 349–353.
- [27] X.L. Li, T.J. Lou, X.M. Sun, Y.D. Li, *Inorg. Chem.* 43 (2004) 5442–5449.
- [28] A. Zaleska, J.W. Sobczak, E. Grabowska, J. Hupka, *Appl. Catal. B* 78 (2008) 92–100.
- [29] K.M. Reddy, S.V. Panorama, A.R. Reddy, *Mater. Chem. Phys.* 78 (2002) 239–245.
- [30] V. Štengl, V. Houšková, S. Bakardjieva, N. Murafa, *Appl. Mater. Interfaces* 2 (2010) 575–580.